Article

# Zirconocene-Catalyzed Propene Polymerization: A Quenched-Flow Kinetic Study

Fuquan Song, Roderick D. Cannon, and Manfred Bochmann

*J. Am. Chem. Soc.*, **2003**, 125 (25), 7641-7653• DOI: 10.1021/ja029150v • Publication Date (Web): 31 May 2003



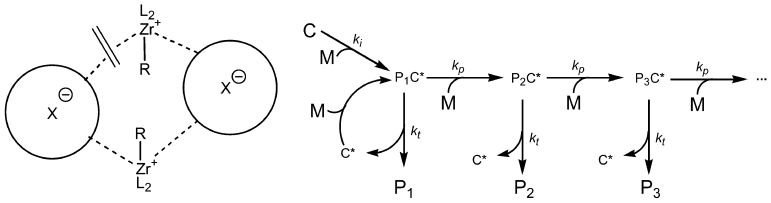


## More About This Article

Additional resources and features associated with this article are available within the HTML version:

- Supporting Information
- Links to the 9 articles that cite this article, as of the time of this article download
- Access to high resolution figures
- Links to articles and content related to this article
- Copyright permission to reproduce figures and/or text from this article

View the Full Text HTML

J|A|C|S
ARTICLES
Published on Web 05/31/2003

# Zirconocene-Catalyzed Propene Polymerization: A Quenched-Flow Kinetic Study

Fuquan Song, Roderick D. Cannon,* and Manfred Bochmann*

*Contribution from the Wolfson Materials and Catalysis Centre, School of Chemical Sciences, University of East Anglia, Norwich NR4 7TJ, United Kingdom*

Received October 30, 2002; E-mail: m.bochmann@uea.ac.uk

***Abstract:*** The kinetics of propene polymerization catalyzed by *ansa*-metallocenes were studied using quenched-flow techniques. Two catalyst systems were investigated, (SBI)$ZrMe_2$/Al$^i$Bu$_3$/[$Ph_3C$][CN{B($C_6F_5$)$_3$}$_2$] (1:100:1) at 25.0 °C and (SBI)$ZrCl_2$/methylalumoxane at 40.0 °C (Al:Zr = 2400:1) (SBI = *rac*-$Me_2$Si(1-Indenyl)$_2$). The aims of the study were to address fundamental mechanistic aspects of metallocene-catalyzed alkene polymerizations, catalyst initiation, the quantitative correlation between catalyst structure and the rate of chain propagation, and the nature of dormant states. One of the most important but largely unknown factors in metallocene catalysis is the distribution of the catalyst between dormant states and species actively involved in polymer chain growth. Measurements of polymer yield $Y$ versus reaction time $t$ for propene concentrations [M] = 0.15−0.59 mol L$^{-1}$ and zirconocene concentrations in the range [Zr] = (2.38−9.52) × 10$^{-5}$ mol L$^{-1}$ for the borate system showed first-order dependence on [M] and [Zr]. Up to $t \approx 1$ s, the half-life of catalyst initiation is comparable to the half-life of chain growth; that is, this phase is governed by non-steady-state kinetics. We propose a rate law which takes account of this and accurately describes the initial rates. Curve fitting of $Y(t)$ data provides an apparent chain growth rate constant $k_p^{app}$ on the order of 10$^3$ L mol$^{-1}$ s$^{-1}$. By contrast, the evolution with time of the number-average polymer molecular weight, which is independent of the concentration of catalyst involved, leads to a $k_p$ which is an order of magnitude larger, (17.2 ± 1.4) × 10$^3$ L mol$^{-1}$ s$^{-1}$. The ratio $k_p^{app}/k_p = 0.08$ indicates that under the given conditions only about 8% of the total catalyst is actively engaged in chain growth at any one time. The system (SBI)$ZrCl_2$/methylalumoxane is significantly less active, $k_p^{app}$ = 48.4 ± 2.7 and $k_p$ = (6 ± 2) × 10$^2$ L mol$^{-1}$ s$^{-1}$, while, surprisingly, the mole fraction of active species is essentially identical, 8%. Evidently, the energetics of the chain growth sequence are strongly modulated by the nature of the counteranion. Increasing the counteranion/zirconium ratio from 1:1 to 20:1 has no influence on catalyst activity. These findings are consistent with a model of closely associated ion pairs throughout the chain growth sequence. For the borate system, propagation is ∼6000 times faster than initiation, while for the MAO catalyst, $k_p/k_i \approx 800$. Polymers obtained at 25 °C show 0.1−0.2 mol % 2,1-regioerrors, and end-group analysis identifies 2,1-misinsertions as the main cause for chain termination (66%), as compared to 34% for the vinylidene end groups. The results suggest that 2,1-regioerrors are a major contributor to the formation of dormant species, even at short reaction times.

## Introduction

Metallocene-based olefin polymerization catalysts have in recent years revolutionized polyolefin production and have dramatically extended the range of polymeric materials that is now available.[1] Apart from their industrial impact, soluble metallocene systems, and in particular "well-defined" catalyst systems based on metallocene alkyls activated with borate-based cation generating agents,[2] have significantly advanced the mechanistic understanding of polymerization processes.[3] Extensive structural modification of the metallocene ligand framework has permitted the construction of a wide range of catalysts with different stereo- and regioselectivities and activities.[4] Despite this, there are remarkably few studies on the kinetic behavior of this important class of catalysts, and little is known about the rate laws that govern catalyst initiation, polymer chain growth, and termination.

(1) (a) Kaminsky, W.; Laban, A. *Appl. Catal.* **2001**, *222*, 47. (b) Tullo, A. H. *Chem. Eng. News* **2001**, October 22, 35. (c) Lee, M. *Chem. Br.* **1998**, September, 22. (d) Kaminsky, W. *J. Chem. Soc., Dalton Trans.* **1998**, 1413. (e) Kaminsky, W.; Arndt, M. *Adv. Polym. Sci.* **1997**, *127*, 143.

(2) (a) Jordan, R. F.; LaPointe, R. E.; Bajgur, C. S.; Echols, S. F.; Willett, R. *J. Am. Chem. Soc.* **1987**, *109*, 4111. (b) Bochmann, M.; Wilson, L. M.; Hursthouse, M. B.; Short, R. L. *Organometallics* **1987**, *6*, 2556. (c) Bochmann, M.; Wilson, L. M.; Hursthouse, M. B.; Motevalli, M. *Organometallics* **1988**, *7*, 1148. (d) Turner, H. W. Eur. Patent Appl. 0277 004, 1988. (e) Bochmann, M.; Jaggar, A. J.; Nicholls, J. C. *Angew. Chem., Int. Ed. Engl.* **1990**, *29*, 780. (f) Horton, A. D.; Frijns, J. H. G. *Angew. Chem., Int. Ed. Engl.* **1991**, *30*, 1152. (g) Siedle, A. R.; Lamanna, W. M.; Newmark, R. A.; Stevens, J.; Richardson, D. E.; Ryan, M. *Makromol. Chem., Macromol. Symp.* **1993**, *66*, 215. (h) Ewen, J. A.; Elder, M. J. *Makromol. Chem., Macromol. Symp.* **1993**, *66*, 179. (i) Ewen, J. A. *Stud. Surf. Sci. Catal.* **1994**, *89*, 405.

(3) (a) Jordan, R. F. *Adv. Organomet. Chem.* **1991**, *32*, 325. (b) Brintzinger, H. H.; Fischer, D.; Mülhaupt, R.; Rieger, B.; Waymouth, R. *Angew. Chem., Int. Ed. Engl.* **1995**, *34*, 1143. (c) Bochmann, M. *J. Chem. Soc., Dalton Trans.* **1996**, 255. (d) Bochmann, M. *Curr. Opin. Solid State Mater. Sci.* **1997**, *2*, 639. (e) Chen, E. Y. X.; Marks, T. J. *Chem. Rev.* **2000**, *100*, 1391.

(4) (a) Resconi, L.; Cavallo, L.; Fait, A.; Piemontesi, F. *Chem. Rev.* **2000**, *100*, 1253. (b) Coates, G. W. *Chem. Rev.* **2000**, *100*, 1253. (c) McKnight, A. L.; Waymouth, R. M. *Chem. Rev.* **1998**, *98*, 2587. (d) Alt, H. G.; Köppl, A. *Chem. Rev.* **2000**, *100*, 1205.

***Scheme 1.*** Fink's Intermittent Chain Growth Model[5d] [a]

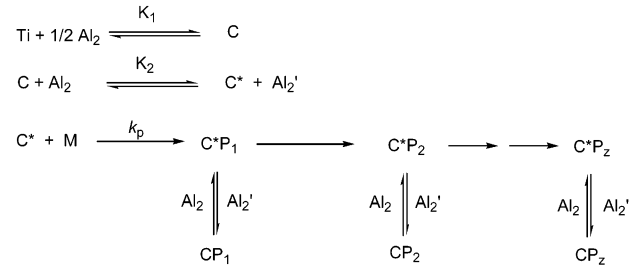


[a] C = catalyst precursor, C* = active $Cp_2TiCl_2/[AlClR_2]_2$ catalyst species, $P_z$ = polymer chain. $C^*P_z$ denotes active species carrying polymeryl chain after *z* monomer insertions, in equilibrium with the resting state $CP_z$.

Investigations on the reaction kinetics of metallocene catalysts to elucidate elementary mechanistic steps in Ziegler−Natta polymerizations were pioneered by Fink and co-workers[5] who used quenched-flow kinetics and $^{13}C$ NMR labeling techniques to study the ethene oligomerization catalyzed by $Cp_2TiRCl/AlR_2Cl$ (R = Me, Et), a relatively slow catalyst system that allowed the determination of the relative rates of first, second, and subsequent ethene insertions into the Ti−Me bond. The authors were able to show that the slowest insertion step is the first monomer insertion; that is, the insertion of $C_2H_4$ into a Ti−Me bond was 120 times slower than that into the Ti−Et bond. Subsequent insertion into higher alkyl−titanium bonds was slower but still significantly faster than the first insertion. The first insertion was rate-determining, and long polymer chains could build up before the majority of the catalyst precursor had been activated. Polymerization was explained by a series of equilibria, the "intermittent growth" model that seems typical of most metallocene polymerization catalysts (Scheme 1). The model assumes that the active species are in equilibrium with observable dormant states which may constitute the bulk of the catalyst, while chain growth resumes at intervals before a termination reaction liberates the polymer chain.[5e] The kinetic behavior of metallocene catalysts differs therefore fundamentally from Brookhart's cationic nickel and palladium polymerization catalysts where the resting state is the ethene complex $[L_2M(R)(C_2H_4)]^+$ (M = Ni, Pd; $L_2$ = diazadiene), the alkyl transfer step is zero-order in monomer, and kinetic parameters can be determined directly by spectroscopic methods.[6]

Subsequently, Shiono et al.[7] and Terano and co-workers[8] employed quenched-flow methods to study heterogeneous Ziegler catalysts, while Busico et al.[9] adopted this method for the study of the homogeneous zirconocene catalyst system *rac*-$Me_2Si(2\text{-Me-}4\text{-PhInd})_2ZrCl_2$/methylalumoxane for the polymerization of ethene and propene. Curve fitting suggested an "initiation" process that converts the catalyst precursor into the active species and a second-order propagation rate constant which was ca. $10^2$ times smaller for propene than for ethene. Landis and co-workers have recently studied the kinetics of 1-hexene polymerization with a *rac*-$C_2H_4(Ind)_2ZrMe_2/B(C_6F_5)_3$ catalyst using quenched-flow and deuteriolysis techniques and suggested a molecular interpretation for initiation, propagation, and termination steps.[10]

It is now accepted that the active species in metallocene-based catalysts are electron-deficient 14-electron alkyl complexes $[Cp_2MR]^+$, paired with weakly coordinating anions $X^-$ (M = Ti, Zr, or Hf).[3] In the case of activation by methylalumoxane (MAO),[11] R = Me and $X^-$ = anion derived from methyl ligand abstraction by a Lewis acidic site on MAO, $[MeMAO]^-$, while activation of metallocene dimethyl catalyst precursors with cation-generating activators such as $[CPh_3][B(C_6F_5)_4]$[12] and $B(C_6F_5)_3$[13] give $[B(C_6F_5)_4]^-$ and $[MeB(C_6F_5)_3]^-$ stabilized ion pairs, respectively. The active species is part of a complex set of equilibria where the incoming monomer may compete for the metal coordination site with the solvent, other metal alkyl species, or, most importantly, the counteranion.[12b,14] Anion association, even with "super-weakly" coordinating anions,[15] is particularly important in low-polarity media typically used for olefin polymerization.[16]

Studies on metallocenium borate systems have identified a number of catalyst resting states.[3c,e] Thus, metallocene dimethyls react with $B(C_6F_5)_3$ to give zwitterions of the type $L_2MMe(\mu\text{-}Me)B(C_6F_5)_3$ (L = cyclopentadienyl derivative, M = group 4 metal),[13] which are thought to dissociate under catalytic conditions to some extent into catalytically active ion pairs $[\{L_2MMe(monomer)\}^+\cdots\{MeB(C_6F_5)_3\}^-]$. An equilibrium constant for this process has yet to be determined. As we showed some time ago, the reaction of metallocene dimethyl complexes with $[CPh_3][B(C_6F_5)_4]$ leads primarily to homobinuclear complexes, $[(L_2MMe)_2(\mu\text{-}Me)]^+[B(C_6F_5)_4]^-$,[17] which in some cases are sufficiently stable to allow isolation and structural characterization.[18] Conversion of $[(L_2MMe)_2(\mu\text{-}Me)]^+[B(C_6F_5)_4]^-$ into the mononuclear ion pair $[L_2MMe^+\cdots B(C_6F_5)_4^-]$ is slow; for example, for $L_2$ = *rac*-$Me_2Si(Ind)_2$, it is much slower than chain propagation.[19a] In the presence of $AlMe_3$, the predominant

(5) (a) Schnell, D.; Fink, G. *Angew. Makromol. Chem.* **1974**, *39*, 131. (b) Fink, G.; Zoller, W. *Makromol. Chem.* **1981**, *182*, 3265. (c) Fink, G.; Schnell, D. *Angew. Makromol. Chem.* **1982**, *105*, 31. (d) Mynott, R.; Fink, G.; Fenzl, W. *Angew. Makromol. Chem.* **1987**, *154*, 1. (e) Fink, G.; Fenzl, W.; Mynott, R. *Z. Naturforsch., B* **1985**, *40b*, 158.
(6) (a) Johnson, L. K.; Killian, C. M.; Brookhart, M. *J. Am. Chem. Soc.* **1995**, *117*, 6414. (b) Svejda, S. A.; Johnson, L. K.; Brookhart, M. *J. Am. Chem. Soc.* **1999**, *121*, 10634.
(7) (a) Shiono, T.; Ohgizawa, M; Soga, K. *Polymer* **1994**, *35*, 187. (b) Soga, K.; Ohgizawa, M.; Shiono, T. *Makromol. Chem., Rapid Commun.* **1989**, *10*, 503.
(8) (a) Keii, T.; Terano, M.; Kimura, K.; Ishii, K. *Makromol. Chem., Rapid Commun.* **1987**, *8*, 583. (b) Terano, M.; Kataoka, T.; Keii, T. *J. Mol. Catal.* **1989**, *56*, 203. (c) Terano, M.; Kataoka, T.; Keii, T. *J. Polym. Sci., Part A: Polym. Chem.* **1990**, *28*, 2035. (d) Mori, H.; Tashimo, K.; Terano, M. *Macromol. Rapid Commun.* **1995**, *16*, 651. (e) Mori, H.; Tashino, K.; Terano, M. *Macromol. Chem. Phys.* **1996**, *197*, 895. (f) Mori, H.; Iguchi, H.; Hasebe, K.; Terano, M. *Macromol. Chem. Phys.* **1997**, *198*, 1249.
(9) Busico, V.; Cipullo, R.; Esposito, V. *Macromol. Rapid Commun.* **1999**, *20*, 116.
(10) (a) Liu, Z.; Somsook, E.; Landis, C. R. *J. Am. Chem. Soc.* **2001**, *123*, 2915. (b) Liu, Z.; Somsook, E.; White, C. B.; Rosaaen, K. A.; Landis, C. R. *J. Am. Chem. Soc.* **2001**, *123*, 11193.
(11) (a) Sinn, H.; Kaminsky, W. *Adv. Organomet. Chem.* **1980**, *18*, 99. (b) Harlan, C. J.; Bott, S. G.; Barron, A. R. *J. Am. Chem. Soc.* **1995**, *117*, 6465. (c) Fusco, R.; Longo, L.; Masi, F.; Garbassi, F. *Macromolecules* **1997**, *30*, 7673. (d) Panchenko, V. N.; Zakharov, V. A.; Danilova, I. G.; Paukshtis, E. A.; Zakharov, I. I.; Goncharov, V. G.; Suknev, A. P. *J. Mol. Catal.* **2001**, *174*, 107. (e) Zurek, E.; Ziegler, T. *Organometallics* **2002**, *21*, 83.
(12) (a) Chien, J. C. W.; Tsai, W. M.; Rausch, M. D. *J. Am. Chem. Soc.* **1991**, *113*, 8570. (b) Bochmann, M.; Lancaster, S. J. *J. Organomet. Chem.* **1992**, *434*, C1.
(13) Yang, X.; Stern, C. L.; Marks, T. J. *J. Am. Chem. Soc.* **1994**, *116*, 10015.
(14) Bochmann, M.; Lancaster, S. J.; Hursthouse, M. B.; Malik, K. M. A. *Organometallics* **1994**, *13*, 2235.
(15) (a) Lupinetti, A. J.; Strauss, S. H. *Chemtracts − Inorg. Chem.* **1998**, *11*, 565. (b) Reed, C. A. *Acc. Chem. Res.* **1998**, *31*, 133. (c) Strauss, S. H. *Chem. Rev.* **1993**, *93*, 927.
(16) Beck, S.; Geyer, A.; Brintzinger, H. H. *Chem. Commun.* **1999**, 2477.
(17) (a) Bochmann, M.; Lancaster, S. J. *Angew. Chem., Int. Ed. Engl.* **1994**, *33*, 1634. (b) Bochmann, M.; Lancaster, S. J. *J. Organomet. Chem.* **1995**, *497*, 55. (c) For related $MeB(C_6F_5)_3^-$ complexes, see: Haselwander, T.; Beck, S.; Brintzinger, H. H. In *Ziegler Catalysts*; Fink, G., Mülhaupt, R., Brintzinger, H. H., Eds.; Springer: Berlin, 1995; p 181. Beck, S.; Prosenc, M. H.; Brintzinger, H. H. *J. Mol. Catal. A: Chem.* **1998**, *128*, 41.
(18) Chen, Y. X.; Stern, C. L.; Yang, S.; Marks, T. J. *J. Am. Chem. Soc.* **1996**, *118*, 12451.

***Scheme 2.*** Mechanistic Principles for Catalyst Activation and the Propene Insertion Process

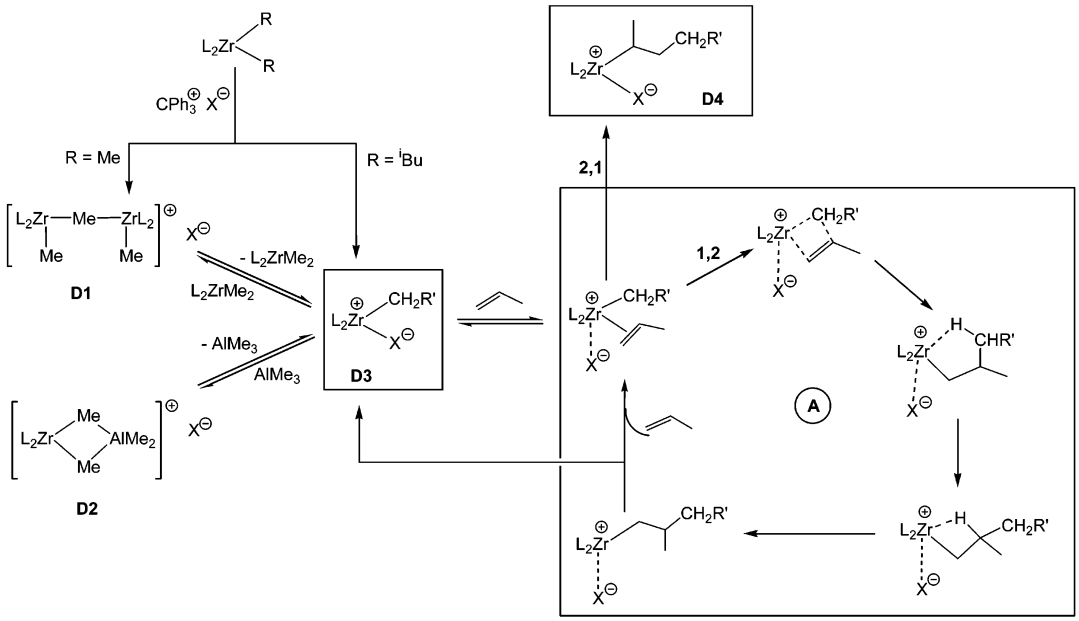


species are heterobinuclear cations, $[L_2M(\mu\text{-}Me)_2AlMe_2]^+$, which are more stable than the homobinuclear complexes.[17] These binuclear compounds have also been identified by NMR spectroscopy in MAO-activated catalyst systems.[20]

A detailed mechanism of the activation process, consistent with these ideas and with the work to be presented here, is shown in Scheme 2. Both methyl-bridged species **D1**, **D2** are regarded as dormant states. While species with methyl-bridges are an important feature of $AlMe_3$- or MAO-containing systems, the stability of $\mu$-alkyl complexes decreases rapidly with increasing bulk of the alkyl group, and in cases where $Cp_2Zr$-$^i$Bu$_2$ precursors or Al$^i$Bu$_3$ scavengers are used, $\mu$-$^i$Bu species are thought to be unimportant.[21] Under such conditions, contact ion pairs are likely to be the dominant resting state **D3**.

It has been shown that the first step in the formation of a catalytically active metallocene species is the monomer association/dissociation preequilibrium to an electron-deficient metallocene species.[22,23] Eventually, alkene binding will be followed by a sequence of steps involved in the alkyl group migration to the coordinated monomer. Together, this multiplicity of states (box A) constitutes the "active species" involved in the chain growth process.

As will be discussed below, different definitions of "active species" have been used in kinetic studies. In particular, the fraction of total metal actively involved in the chain growth process at any one time remained unknown but is of key importance for an understanding of catalyst activity. Eventually, most of the precursor complex (C in Scheme 1) will become involved in the chain growth process. In that sense, all metal species bearing a polymeryl chain can be thought of as active species. With this definition, the ratio of active to inactive catalytic centers will rise toward 1.0 with reaction time (or to a slightly lower figure due to partial catalyst death). In another definition, the term "active species" is defined as comprising species of type **A** in Scheme 2, in which case the mole fraction will remain $\ll 1.0$.

During the propene polymerization process, the monomer can insert either in 1,2- or in 2,1-fashion, to give either a primary or a secondary alkyl product. As Busico has pointed out, although 2,1-insertions are infrequent, the rate for the insertion of another monomer following a 2,1-regioerror is $10^2-10^3$ times slower than for insertion into a primary Zr alkyl bond, and even few 2,1-insertion events can convert a large proportion of the catalyst into dormant species and thus inhibit catalytic activity.[24] In the absence of rapid chain transfer and other reactivation pathways (such as hydrogenolysis), the formation of *sec*-alkyl zirconocene species is therefore likely to be an important deactivation pathway (Scheme 2, state **D4**) and will have a profound influence on polymerization kinetics.

We have recently set out to quantify the factors that govern catalyst activity, such as the contribution of anions to the activation barrier of propene polymerization. Using batch polymerizations with the catalyst system (SBI)$ZrMe_2$/Al$^i$Bu$_3$/$[CPh_3]^+X^-$ (SBI = *rac*-$Me_2Si(Ind)_2$) and extrapolating catalyst activity as a function of the counteranion to zero anion concentration has enabled us to quantify the anion contribution to the activation barrier of zirconocene-catalyzed propene polymerizations,[19] with barriers increasing in the series X = $[CN\{B(C_6F_5)_3\}_2]^-$ < $[H_2N\{B(C_6F_5)_3\}_2]^-$ ≈ $[B(C_6F_5)_4]^-$ ≪ [MeB-

(19) (a) Zhou, J.; Lancaster, S. J.; Walker, D. A.; Beck, S.; Thornton-Pett, M.; Bochmann, M. *J. Am. Chem. Soc.* **2001**, *123*, 223. (b) Lancaster, S. J.; Rodriguez, A.; Lara-Sanchez, A.; Hannant, M. D.; Walker, D. A.; Hughes, D. L.; Bochmann, M. *Organometallics* **2002**, *21*, 451−453.

(20) (a) Tritto, I.; Donetti, R.; Sacchi, M. C.; Locatelli, P.; Zannoni, G. *Macromolecules* **1997**, *30*, 1247. (b) Tritto, I.; Donetti, R.; Sacchi, M. C.; Locatelli, P.; Zannoni, G. *Macromolecules* **1999**, *32*, 264. (c) Babushkin, D. E.; Semikolenova, N. V.; Zakcharov, V. A.; Talsi, E. P. *Macromol. Chem. Phys.* **2000**, *201*, 558. (d) See also: Vanka, K.; Ziegler, T. *Organometallics* **2001**, *20*, 905.

(21) For example, the reaction of $Cp_2Zr^iBu_2$ with $[CPh_3][B(C_6F_5)_4]$ leads to fast formation of $[Cp_2Zr(\eta^3\text{-methallyl})]^+$, without evidence for $\mu$-$^i$Bu intermediates: Carr, A. G.; Dawson, D. M.; Thornton-Pett, M.; Bochmann, M. *Organometallics* **1999**, *18*, 2933.

(22) (a) Karl, J.; Dahlmann, M.; Erker, G.; Bergander, K. *J. Am. Chem. Soc.* **1998**, *120*, 5643. (b) Dahlmann, M.; Erker, G.; Bergander, K. *J. Am. Chem. Soc.* **2000**, *122*, 7986.

(23) (a) Wu, Z.; Jordan, R. F.; Petersen, J. L. *J. Am. Chem. Soc.* **1995**, *117*, 5867. (b) Casey, C. P.; Hallenbeck, S. L.; Pollock, D. W.; Landis, C. R. *J. Am. Chem. Soc.* **1995**, *117*, 9770. (c) Galakhov, M. V.; Heinz, G.; Royo, P. *Chem. Commun.* **1998**, 17. (d) Casey, C. P.; Carpenetti, D. W.; Sakurai, H. *J. Am. Chem. Soc.* **1999**, *121*, 9483.

(24) (a) Busico, V.; Cipullo, R.; Corradini, P. *Makromol. Chem.* **1993**, *194*, 1079. (b) Busico, V.; Cipullo, R.; Corradini, P. *Makromol. Chem., Rapid Commun.* **1993**, *14*, 97. (c) Busico, V.; Cipullo, R.; Chadwick, J. C.; Modder, J. F.; Sudmeijer, O. *Macromolecules* **1994**, *27*, 7538. (d) Busico, V.; Cipullo, R.; Ronca, S. *Macromolecules* **2002**, *35*, 1537.

***Scheme 3***

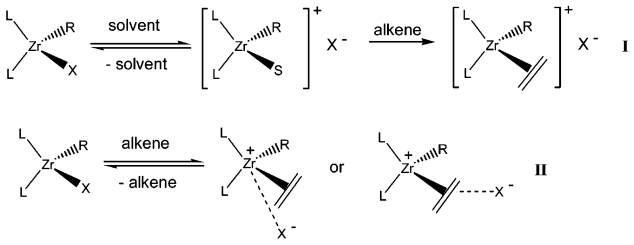


$(C_6F_5)_3$]. Such an effect could have two reasons: (i) catalyst activity is limited by the extent of dissociation of the initial contact ion pair into a solvent-separated ion pair which then picks up a monomer molecule (Scheme 3, model **I**), or (ii) the alkene reacts with the contact ion pair with associative displacement of the anion to give a monomer-separated ion pair (model **II**). In model **II**, one may expect the anion to remain sufficiently closely involved to influence subsequent migratory alkene insertion events. Theoretical approaches suggest the latter to be energetically favored.[25] The current study was undertaken partly to seek clarification of this point, and we now report here the results of a kinetic study of this system using quenched-flow methods.

## Experimental Section

**Materials.** All manipulations were performed under dry nitrogen gas using standard Schlenk techniques. Solvents were purified by distillation under nitrogen from sodium−potassium (light petroleum, bp 40−60 °C) or sodium (low-sulfur toluene). Propene (BOC, 99%) was dried by passing through a column packed with supported $P_2O_5$ with moisture indicator, followed by a column of 4 Å molecular sieves. The compounds (SBI)$ZrMe_2$ (SBI = *rac*-$Me_2Si$(1-Indenyl)$_2$),[14,26] [$Ph_3C$][$B(C_6F_5)_4$],[12] and [$Ph_3C$][$CN\{B(C_6F_5)_3\}_2$][27] were made according to published methods and stored as solids in a drybox under nitrogen at room temperature. The compound $[C_6H_5CH_2NEt_3]^+[B(C_6F_5)_4]^-$ was synthesized by reaction of $[C_6H_5CH_2NEt_3]^+Br^-$ with Li$[B(C_6F_5)_4]$ in dichloromethane and purified by recrystallization from dichloromethane/light petroleum (1:4). Li$[B(C_6F_5)_4]$ was made from $B(C_6F_5)_3$ and $LiC_6F_5$ in petroleum ether and was free from other borate impurities within NMR detection limits. Solutions of triisobutyl aluminum were made by dissolving the required amount of neat $Al^iBu_3$ (Aldrich) in toluene in a large Schlenk tube. Methylalumoxane (MAO) in toluene (Witco) was specified as containing 6−8% weight % MAO and 2−4% weight % $AlMe_3$.

**Apparatus.** $^1H$ NMR and $^{13}C$ NMR spectra were recorded on a Bruker Avance DPX300 spectrometer. Chemical shifts were referenced to residual solvent peaks. Curve fitting was carried out using Origin 6.1 Scientific Graphing and Analysis software.

A schematic representation of the quenched-flow apparatus is shown in Figure 1. (A) and (B) are, respectively, reservoirs for neat toluene and for toluene solutions of propene, both thermostated to 25 ± 0.1 °C (Haake C10-K10 water bath, nominal accuracy ±0.04 °C), while the temperature of the whole apparatus was controlled to 25 ± 1 °C by air conditioning. Both reservoirs are connected to a three-way Swagelock valve (D) that allows either purging with neat toluene or delivery of monomer solution to syringe (C). Syringe (C) is a 100 mL Hamilton gastight syringe with Teflon plunger, driven by a stepless syringe pump with programmable flow rates from 220 mL/min to

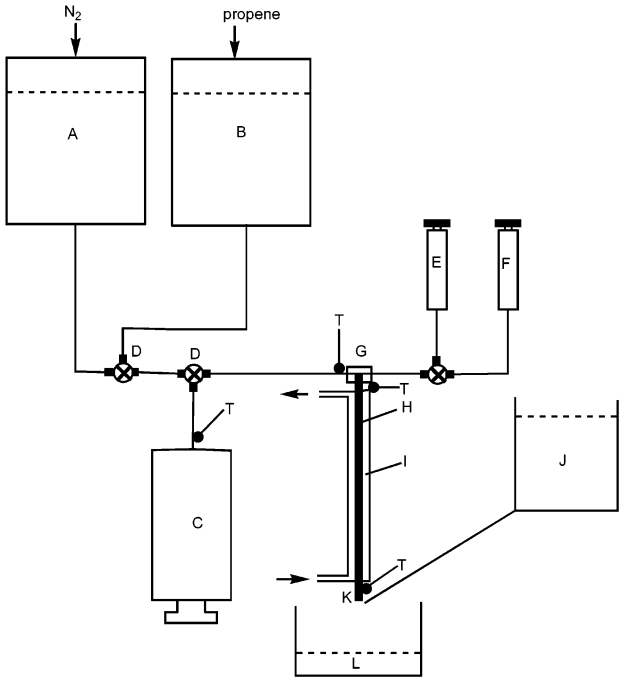


***Figure 1.*** Schematic representation of quenched-flow apparatus. (A) Jacketed and thermostated (25 °C) toluene reservoir. (B) Jacketed and thermostated (25 °C) reservoir containing toluene saturated with 1 bar of propene. (C) 100 mL syringe with monomer solution. (D) Swagelock valves. (E) $L_2ZrMe_2/Al^iBu_3$ 1:7 in toluene. (F) Catalyst activator in toluene. (G) Mixing chamber. (H) 14-gauge stainless steel tube reactor. (I) Thermostated jacket connected to a water bath. (J) Methanol reservoir. (K) Quenching point. (L) Collecting vessel with acidified methanol. T denotes attachment points for thermocouples for temperature control.

0.0001 μL/h, with an accuracy of ±1% and reproducibility of ±0.1% (Harward Apparatus Co., model PHD2000 with infusion/withdraw modes). The precatalyst plus scavenger (E) and cocatalyst solutions (F) are contained in 10 mL Hamilton gastight precision glass syringes with Teflon plungers, driven simultaneously by a second stepless syringe pump (PHD2000). Connecting tubes are 16-gauge stainless steel connected with T-pieces with Luer fittings. The mixing chamber (G) is constructed from glass capillary tubing of 1 mm i.d., with Luer fittings and a dead volume of 1 μL, corresponding to a dead time of ca. 1 ms (calculated for a typical flow rate of 42 mL $min^{-1}$). Polymerization starts at (G) and is quenched at junction (K).

The reactor tube (H) was either 10−19 gauge stainless steel with lengths of 12−24 in. or, for preliminary experiments only, 14-gauge Teflon tubing. The reactor tube was surrounded by a water jacket (I) connected to a thermostated water bath (Haake C10-K10, 25 ± 0.1 °C). The quenching agent in reservoir (J) is a solution of HCl (0.1 M) and water (0.5 M) in methanol, running continuously from a tube of the same diameter as the reactor tube. The two solutions were arranged to cross at right angles in open air, a few millimeters from the respective outlets, which are enclosed within a larger glass tube. This arrangement was found to satisfactorily avoid clogging of the flow lines with solid polymer.

**Propene Polymerizations with (SBI)$ZrMe_2$/[$Ph_3C$][$CN\{B(C_6F_5)_3\}_2$].** Stock solutions of the catalyst precursor were made by dissolving (SBI)-$ZrMe_2$ in the required volume of toluene together with $Al^iBu_3$ (Al:Zr = 7:1). Because dilute solutions of metallocenes were found to deteriorate despite stringent precautions, fresh stock solutions were prepared for each set of experiments. All measurements were conducted with metallocene solutions that were less than 2 h old. Propene solutions were prepared by thermostating 1 L of toluene containing 2 mmol of $Al^iBu_3$ at 25 ± 0.1 °C under 1 bar of propene for 3 h ([M] = 0.62 mol $L^{-1}$).

(25) (a) Lanza, G.; Fragalà, I. L. *Top. Catal.* **1999**, *7*, 45. (b) Chan, M. S. W.; Vanka, K.; Pye, C. C.; Ziegler, T. *Organometallics* **1999**, *18*, 4624. (c) Vanka, V.; Chan, M. S. W.; Pye, C. C.; Ziegler, T. *Organometallics* **2000**, *19*, 1841.
(26) Kim, I, Zhou, J. *J. Polym. Sci., Part A. Polym. Chem.* **1999**, *37*, 1071.
(27) Lancaster, S. J.; Walker, D. A.; Thornton-Pett, M.; Bochmann, M. *Chem. Commun.* **1999**, 1533.

***Table 1.*** Polypropylene Yields *Y* as Functions of Reaction Time *t* for the Borate-Based Catalyst System[a]

| *t*/s | *Y*/g | | | | | | |
|---|---|---|---|---|---|---|---|
| $[C]_T/10^{-5}$ mol $L^{-1}$: | 2.38[b] | 4.76[c] | 7.14[c] | 9.52[d] | 9.52[b] | 9.52[b] | 9.52[b] |
| $[M]_0$/mol $L^{-1}$: | 0.59 | 0.59 | 0.59 | 0.59 | 0.44 | 0.30 | 0.15 |
| 0.2337 | 0.0027 ± 0.0001 | 0.0058 ± 0.0003 | 0.0149 ± 0.0009 | 0.0191 ± 0.0009 | 0.0175 ± 0.0005 | 0.0119 ± 0.0002 | 0.0074 ± 0.0003 |
| 0.3069 | 0.0038 ± 0.0003 | 0.0094 ± 0.0007 | 0.0209 ± 0.0013 | 0.0259 ± 0.0015 | 0.0230 ± 0.0012 | 0.0172 ± 0.0002 | 0.0107 ± 0.0008 |
| 0.4511 | 0.0058 ± 0.0003 | 0.0170 ± 0.0013 | 0.0332 ± 0.0018 | 0.0440 ± 0.0024 | 0.0367 ± 0.0029 | 0.0280 ± 0.0014 | 0.0149 ± 0.0012 |
| 0.5566 | 0.0079 ± 0.0006 | 0.0233 ± 0.0016 | 0.0436 ± 0.0020 | 0.0590 ± 0.0022 | 0.0480 ± 0.0040 | 0.0355 ± 0.0012 | 0.0190 ± 0.0010 |
| 0.7157 | 0.0124 ± 0.0010 | 0.0323 ± 0.0022 | 0.0642 ± 0.0037 | 0.0796 ± 0.0033 | 0.0634 ± 0.0027 | 0.0453 ± 0.0020 | 0.0233 ± 0.0017 |
| 0.9552 | 0.0191 ± 0.0014 | 0.0485 ± 0.0030 | 0.0920 ± 0.0052 | 0.1190 ± 0.0054 | 0.0897 ± 0.0085 | 0.0618 ± 0.0015 | 0.0288 ± 0.0026 |
| 1.1823 | 0.0273 ± 0.0021 | 0.0676 ± 0.0046 | 0.1163 ± 0.0074 | 0.1575 ± 0.0051 | 0.1095 ± 0.0085 | 0.0774 ± 0.0012 | 0.0336 ± 0.0021 |
| 1.6995 | 0.0458 ± 0.0033 | 0.1033 ± 0.0069 | 0.1648 ± 0.0101 | 0.2287 ± 0.0085 | 0.1635 ± 0.0093 | 0.1090 ± 0.0015 | 0.0477 ± 0.0025 |
| 2.5016 | 0.0837 ± 0.0062 | 0.1570 ± 0.0080 | 0.2342 ± 0.0144 | 0.3062 ± 0.0108 | 0.2230 ± 0.0178 | 0.1538 ± 0.0017 | 0.0651 ± 0.0024 |
| 3.2251 | | | | 0.3790 | | | |
| 3.9636 | | | | 0.4303 | | | |
| 5.2257 | | | | 0.5340 | | | |

[a] (SBI)$ZrMe_2$/Al$^i$$Bu_3$/[$Ph_3C$][CN{B($C_6F_5$)$_3$}$_2$] (1:100:1), 25.0 °C, toluene. Values listed are averages of the specified number of experiments, with standard errors of estimate. [b] Average of five experiments. [c] Average of seven experiments. [d] Average of 10 experiments.

The glass reservoirs (A) and (B) were connected to a Schlenk line for anaerobic operation. The propene solution was drawn into syringe (C) by means of the syringe pump, but with a small positive propene pressure applied at (B). Propene concentrations were varied by diluting a toluene solution saturated with propene at 25 ± 0.1 °C with additional toluene, to give monomer concentrations [M] of 0.15−0.59 mol $L^{-1}$, while the zirconocene concentration was varied over the range (2.38−9.52) × $10^{-5}$ mol $L^{-1}$. Flow rates were 40 mL $min^{-1}$ (monomer) and 1 mL $min^{-1}$ each for catalyst and activator, to give a total flow rate of 42 mL $min^{-1}$, which was kept constant for this series of experiments. Collection time was 1 min. At the quenching point, the ratio of methanol to toluene was about 1.5:1. The quenched solution was collected in a beaker (L) containing excess methanol. Reaction times were varied by selecting appropriate tube lengths and diameters. When different combinations of lengths and diameters were selected to give the same flow rate, yields were typically consistent within ±5%. In a typical run, the total volume of solution passed was sufficient to produce about 0.01−0.3 g of polymer, and the volume of quench solution was about 200 mL. The polymer was collected by filtration on a no. 4 glass sinter filter, washed with methanol, and dried overnight at 100 °C. Each experiment was generally repeated 4−10 times. Reproducibility was typically ±5%. After each run, the reactor tube was cleaned out with hot toluene to remove a thin surface layer of polymer deposit.

The progress of the reaction, defined as change in monomer concentration, was calculated using

$$[M]_0 - [M] = Y/Vm_M$$

where $[M]_0$ and [M] are the concentrations of propene at reaction times 0 and *t*, *Y* is the yield (mass) of polymer collected from the solution volume *V*, and $m_M$ is the monomer molecular weight. The results are collected in Table 1.

**Polymerizations with (SBI)$ZrCl_2$/MAO.** A catalyst stock solution of [Zr] = 6.0 × $10^{-3}$ mol $L^{-1}$ was prepared by dissolving (SBI)$ZrCl_2$ (81.0 mg, 0.18 mmol) in 30 mL of MAO in toluene (Al content 1.5 mol $L^{-1}$). This solution was allowed to age for 30 min at room temperature prior to polymerization. The monomer solution was prepared by saturating a mixture of 200 mL of MAO solution and 1 L of toluene (final [Al] = 0.36 mol $L^{-1}$) with propene at 40 °C. The polymerization was conducted at 40 °C, with flow rates of 10 mL/min (monomer) and 0.25 mL/min (catalyst), with a collection time of 8 min. The Al:Zr ratio was 2400:1. Polymerizations were conducted at nine different polymerization times using nine different stainless steel needle reactors (gauge × in.: 16 × 12, 15 × 12, 14 × 12, 13 × 12, 12 × 12, 12 × 18, 12 × 24, 11 × 24, 10 × 24). The collecting time of each experiment was 8 min.

**Polymer Analysis.** Polymer molecular weights were determined by gel permeation chromatography in 1,2,4-trichlorobenzene with antioxidant at 160 °C using a Polymer Laboratories GPC220 instrument equipped with a refractive index and a PD2040 light scattering detector and equipped with two PLGel mixed-B columns. Some samples were determined at 140 °C using the refractive index detector only, relative to polystyrene standards. $^1$H NMR spectra were recorded in $CDCl_3$ at 70 °C, and $^{13}$C NMR spectra were recorded in 1,2,4-$C_6H_3Cl_3$/$C_6D_6$ at 120 °C. Samples showed relative *mmmm* pentad intensities of 95% and 90% for samples obtained at 25 and 40 °C, respectively.

## Results

**Borate-Activated Catalyst System.** The kinetics of propene polymerization using the catalyst system (SBI)$ZrMe_2$/Al$^i$$Bu_3$/[$Ph_3C$][CN{B($C_6F_5$)$_3$}$_2$] (1:100:1)[18] were measured at 25.0 ± 0.1 °C in a purpose-built quenched-flow apparatus depicted in Figure 1. The zirconocene stock solutions contained 7 mol equiv of triisobutylaluminum as transalkylation reactant and scavenging agent. NMR studies have shown that at this Al/Zr ratio all zirconocene methyl ligands are exchanged for isobutyl, within NMR detection limits. We make the assumption that the subsequent reaction with [$Ph_3C$][CN{B($C_6F_5$)$_3$}$_2$] to generate [(SBI)Zr$^i$$Bu^+$···CN{B($C_6F_5$)$_3$}$_2^-$] ion pairs is complete by the time the mixture of catalyst precursor and trityl salt solutions has reached the mixing chamber of the quenched-flow apparatus (≤0.5 s). Under such conditions, the presence of methyl ligands is thought not to be important, so that the participation of methyl-bridged species (Scheme 2, **D1** and **D2**) can be neglected. The monomer was supplied as a toluene solution thermostated at the reaction temperature and containing additional Al$^i$$Bu_3$, to give an overall Al:Zr molar ratio of 100:1. Polymerizations were conducted using jacketed thermostated stainless steel tube reactors to give reaction times from 0.2 to ca. 8 s.

**Reaction Order.** Polymerization reactions are generally described by the empirical rate law:

$$\text{rate} = -\frac{d[M]}{dt} = k[C][M]^{\alpha} \qquad (1)$$

where [M] is the monomer concentration, [C] is the catalyst concentration (variously defined), *t* is the reaction time, and *k* is a rate constant, generally taken to be the chain propagation rate constant. Although most polymerizations are first-order in monomer, in some instances, a noninteger dependence on [M] has been found, $0 < \alpha < 2$. Values of $\alpha > 1$ in some systems

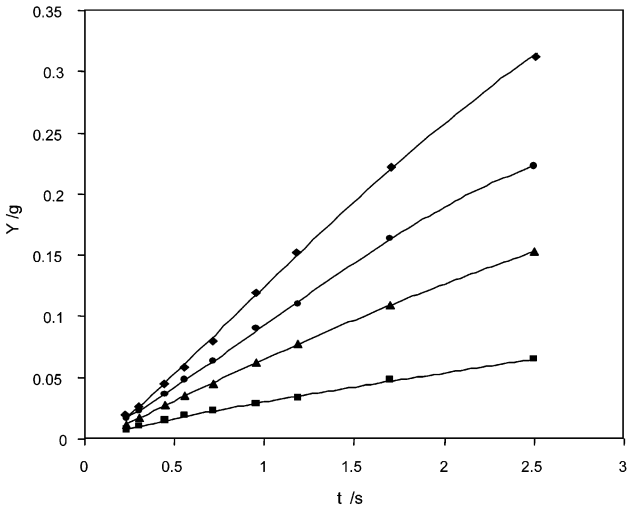


***Figure 2.*** Time-dependence of polymer yield for different initial monomer concentrations. [Zr] = $9.52 \times 10^{-5}$ mol $L^{-1}$; $T = 25$ °C. $[M]_0 = 0.15$ (■), 0.30 (▲), 0.44 (●), and 0.59 mol $L^{-1}$ (◆).

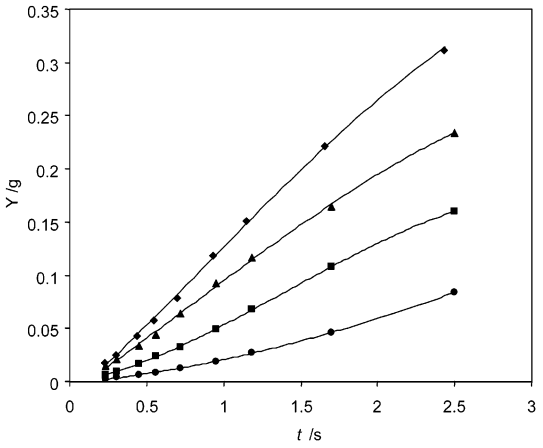


***Figure 3.*** Time-dependence of polymer yield for different catalyst concentrations. $[M]_0 = 0.59$ mol $L^{-1}$; $T = 25$ °C. $[C]_T = [Zr] = 2.38$ (●), 4.76 (■), 7.14 (▲), and $9.52 \times 10^{-5}$ mol $L^{-1}$ (◆).

have led to the hypothesis that a second monomer molecule may the involved in the transition state.[28,29]

In the present system, typical plots of yield against time for quenching times up to about 2.5 s are shown in Figures 2 and 3.

Negative curvature (deceleration) at longer reaction times and/or higher catalyst concentrations is consistent with depletion in monomer, while positive curvature (acceleration) at shorter reaction times is accounted for by the mechanism presented below. Curves fitted using the expression $Y = A + Bt + Ct^2$ extrapolated satisfactorily to the origin, with values of $A$ in the range zero ± two standard errors of estimate, with no initial time delay greater than the experimental error of ±0.03 s. An example is shown in Figure 4. Plots of initial rates (i.e., the

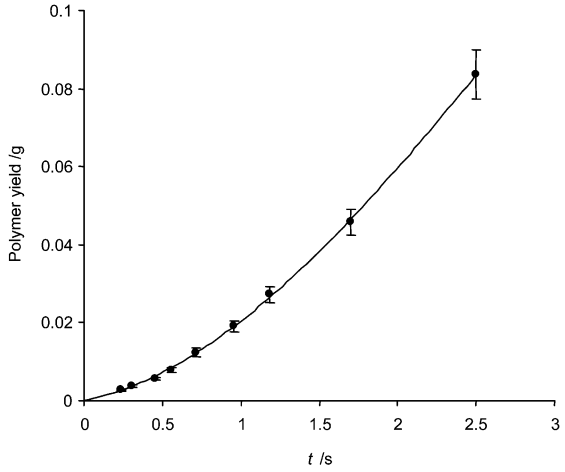


***Figure 4.*** Time-dependence of polymer yield. $[C]_T = [Zr] = 2.38 \times 10^{-5}$ mol $L^{-1}$; $[M]_0 = 0.59$ mol $L^{-1}$; $T = 25.0$ °C. Each point represents an average of the yields observed for a given time, as shown in Table 1.

parameter $B$ estimated in this way) versus initial monomer concentration $[M]_0$ and total catalyst concentration $[C]_T$ are shown in Figure 5.[30] They support the expression

$$R_0 = (-\mathrm{d}[M]/\mathrm{d}t)_{t=0} = k[M]_0[C]_T \qquad (2)$$

and confirm that, in eq 1, $\alpha = 1$ in the present case.

**The Polymerization Mechanism.** The stoichiometric mechanism we use to rationalize these data is shown in Scheme 4.

We assume that the catalyst precursor C reacts with the monomer M with an initiation rate constant $k_i$ to generate an active species $P_1C^*$, consisting of an active center carrying an incipient polymer chain $P_1$. No further assumption is made at this stage about the nature of the initiation process or the structure of $P_1C^*$. It is also assumed that the propagation rate constants $k_p$ for subsequent monomer insertion events are identical. All species $P_zC^*$ ($z = 1, 2, \ldots$) contain essentially the same active center with the polymeryl chain containing $z$ units of monomer. As compared to our detailed Scheme 2, above, C corresponds to the catalyst species on the left of the scheme, and $P_zC^*$ corresponds to the aggregate of active species in box A. Finally, we assume that irreversible chain termination steps proceed from any of the species $P_zC^*$ with identical rates $k_t$ to release the unreactive polymer $P_z$ and the active catalyst C*, which is assumed to react rapidly and completely with monomer to start a new polymer chain. These termination steps are not shown in Scheme 2.

With this scheme, the growth of the total active species is given by

$$\frac{\mathrm{d}[C^*]}{\mathrm{d}t} = k_i[M][C] \qquad (3a)$$

$$[C^*] = [C]_T(1 - e^{-k_i[M]_0 t}) \qquad (3b)$$

where $[C]_T$ is the total zirconocene concentration $[C] + [C^*] = [C] + \sum[P_zC^*]$, and [C] is the concentration of nonactive catalyst. For low conversions, we neglect the change of [M]

(28) (a) Nerfert, N.; Fink, G. *Makromol. Chem., Macromol. Symp.* **1993**, *66*, 157. (b) Jüngling, S.; Mülhaupt, R.; Stehling, U.; Brintzinger, H. H.; Fischer, D.; Langhauser, F. *Makromol. Chem., Macromol. Symp.* **1995**, *97*, 205.

(29) (a) Ystenes, M. *J. Catal.* **1991**, *129*, 383. (b) Thorshaug, K.; Støvneng, J. A.; Rytter, E.; Ystenes, M. *Macromolecules* **1998**, *31*, 7149. (c) Muñoz-Escalona, Ramos, J.; Cruz, V.; Martinez-Salazar, J. *J. Polym. Sci., Part A: Polym. Chem.* **2000**, *38*, 571.

(30) The positive intercept in Figure 5b is assumed to be due to loss of catalyst, for example, by deactivation with unscavanged impurities at a level of ca. $1.7 \times 10^{-5}$ mol $L^{-1}$.

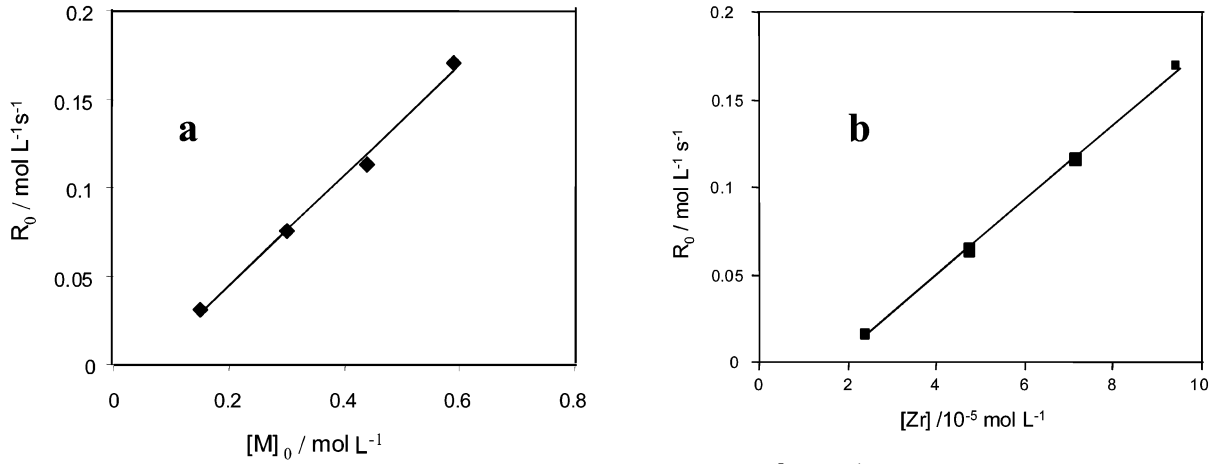


***Figure 5.*** (a) Dependence of initial rate $R_0$ (eq 2) on monomer concentration. [Zr] = 9.5 × 10$^{-5}$ mol L$^{-1}$; $T$ = 25.0 °C. (b) Dependence of initial rate on total zirconocene concentration. [M]$_0$ = 0.59 mol L$^{-1}$; $T$ = 25.0 °C.

***Scheme 4.*** Proposed Mechanistic Scheme for the Polymerization Reaction

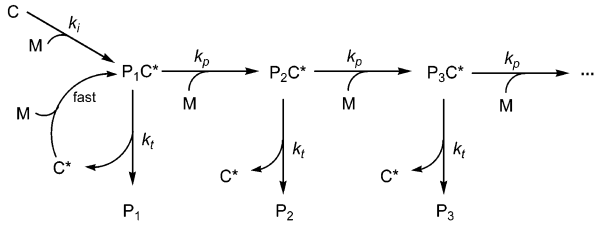


over this time scale. The rate of monomer conversion is given by

$$-\mathrm{d[M]}/\mathrm{d}t = k_i[\mathrm{M}][\mathrm{C}] + (k_p[\mathrm{M}] + k_t)([\mathrm{P_1C^*}] + [\mathrm{P_2C^*}] + \ldots.)$$
$$= k_i[\mathrm{M}]_0[\mathrm{C}] + (k_p[\mathrm{M}]_0 + k_t)[\mathrm{C^*}]$$
$$= (k_p[\mathrm{M}]_0 + k_t)[\mathrm{C}]_T + k_i[\mathrm{M}]_0 - k_p[\mathrm{M}]_0 - k_t[\mathrm{C}]_T e^{-k_i[\mathrm{M}]_0 t} \quad (4)$$

This can be integrated to give eq 5:

$$[\mathrm{M}]_0 - [\mathrm{M}] = [\mathrm{C}]_T(k_p[\mathrm{M}]_0 + k_t)t + \frac{[\mathrm{C}]_T(k_i[\mathrm{M}]_0 - k_p[\mathrm{M}]_0 - k_t)}{k_i[\mathrm{M}]_0}(1 - e^{-k_i[\mathrm{M}]_0 t}) \quad (5)$$

Given that in practice $k_i \ll k_p$ and $k_t \ll k_p[\mathrm{M}]_0$, eq 5 reduces to

$$[\mathrm{M}]_0 - [\mathrm{M}] = k_p[\mathrm{M}]_0[\mathrm{C}]_T\, t\left(1 - \frac{1 - e^{-k_i[\mathrm{M}]_0 t}}{k_i[\mathrm{M}]_0 t}\right) \quad (6)$$

In the limit of $t = 0$, it gives $-\mathrm{d[M]}/\mathrm{d}t = k_i[\mathrm{M}]_0[\mathrm{C}]_T$, but in the limit of $k_i[\mathrm{M}]_0 t \to \infty$, it gives $-\mathrm{d[M]}/\mathrm{d}t = k_p[\mathrm{M}]_0[\mathrm{C}]_T$. Thus, in the evolution of yield with time, the role of $k_i$ is to provide an initial reaction phase, after which the rate law becomes as in eq 2, with the empirical rate constant identified as $k = k_p$.

As we show below, an initial phase can in fact be detected, but it becomes insignificant at times longer than about 0.5 s. Over the main reaction phase, up to $t$ = 5 s, the kinetics are pseudo-first-order in monomer. Fitting the data to eq 5 provides an estimate of $k_p$.[31] For the range of catalyst concentrations listed in Table 1, $k_p \approx (1.3-1.9 \pm 0.1) \times 10^3$ L mol$^{-1}$ s$^{-1}$, with the lower values found for the higher catalyst concentration where monomer depletion effects are felt.

The initiation rate constant is more difficult to determine with accuracy. Because the influence of the initiation process is most pronounced at the very early stages of the reaction where few data points are available, it was important to test the validity of the curve fitting approach. The effect of the initiation phase is seen most clearly in Figure 6, where representative polymer yield data for the (SBI)ZrMe$_2$/Al$^i$Bu$_3$/[Ph$_3$C][CN{B(C$_6$F$_5$)$_3$}$_2$] catalyst are superimposed, with no averaging, but with each experiment normalized with respect to the final limiting slope: all of the data deviate from linearity at short reaction times, as would be expected during catalyst initiation. Evaluating the half-life $t_{1/2}^{\mathrm{init}}$ for this initial phase in a series of about 20 such curves provides $t_{1/2}^{\mathrm{init}} = 0.24 \pm 0.03$ s, $k_i^{\mathrm{obs}} = \ln(2)/t_{1/2}^{\mathrm{init}} = 2.9 \pm 0.4$ s, and $k_i = k_i^{\mathrm{obs}}/[\mathrm{M}]_0 = 5.2 \pm 0.6$ mol$^{-1}$ L$^{-1}$ s, where we have used the average value of [M]$_0$ = 0.56 mol L$^{-1}$ over all of the experiments.[32]

**Polymer Molecular Weights.** The molecular weights of polypropene obtained with the (SBI)ZrMe$_2$/Al$^i$Bu$_3$/[Ph$_3$C][(C$_6$F$_5$)$_3$BCNB(C$_6$F$_5$)$_3$] system as a function of reaction time are shown in Table 2 and Figure 7. They show a sharp increase over the early stages of polymerization, up to $t \approx 1.5$ s, followed by a leveling at $\bar{M}_n \approx 4.4 \times 10^4$ up to 5 s, the longest polymerization time employed for this set of experiments. Even at these early stages, the polymerization is not living, as indicated by the polydispersity and the observation of unsaturated polymer end groups by $^1$H NMR spectroscopy (vide infra). At reaction times of 1 s, on average, about 0.7−1.0 polymer chains are produced per metal center, rising to ca. 1.8 per Zr at 5 s, implying that chain transfer to aluminum is negligible.

In our notation, the number-average molecular weight $\bar{M}_n$ and the number-average degree of polymerization $\langle n \rangle$ are given by

$$\langle n \rangle = \frac{\overline{M_n}}{m_M} = \frac{\sum z\mathrm{P}_z}{\sum \mathrm{P}_z} \quad (7)$$

where $m_M$ is the monomer molecular weight ($z$ = 1, 2, 3, . . .). Because from our kinetic scheme the rate of formation of polymer $\mathrm{P}_z$ is given by $\mathrm{d[P}_z\mathrm{]}/\mathrm{d}t = k_t[\mathrm{P}_z\mathrm{C^*}]$, at time $t$ we have

$$[\mathrm{P}_z] = k_t \int_0^t [\mathrm{P}_z\mathrm{C^*}]\, \mathrm{d}t \quad (8)$$

and finally

(31) $k_t$ is too small as compared to $k_p$ to be determined by this method.

$$\langle n\rangle = \frac{\dfrac{(k_p[M]_0 + k_t)t}{k_t} + \dfrac{k_p[M]_0 + k_t - k_i[M]_0}{k_i[M]_0(k_t - k_i[M]_0)}\left(e^{-k_i[M]_0 t} - 1\right) - \dfrac{k_p[M]_0 + k_i[M]_0}{k_t^2(k_t - k_i[M]_0)}\left(e^{-k_t t} - 1\right)}{t + \dfrac{1}{k_i[M]_0}e^{-k_i[M]_0 t} - \dfrac{1}{k_i[M]_0}} \tag{9}$$

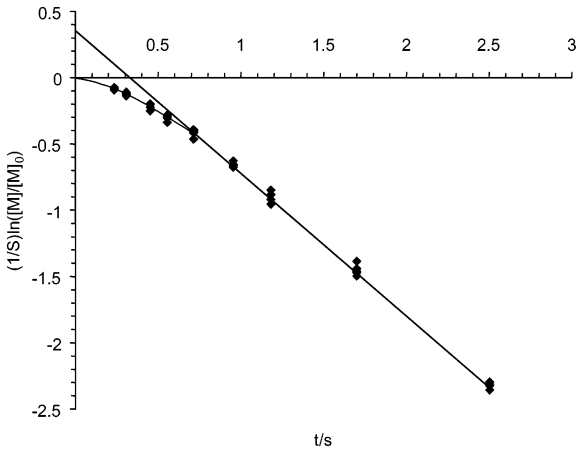


***Figure 6.*** Slope-normalized logarithmic plots. Each data point represents the quantity $S^{-1}\ln\{[M]/[M]_0\}$, calculated from plots of ln[M] versus time, where $S$ is the limiting slope as $t \rightarrow \infty$. Data are superimposed for representative catalyst and monomer concentrations. The deviations from linearity at short reaction times reflect the first kinetic phase of the reaction.

***Table 2.*** Polypropene Molecular Weights (GPC) in the Borate-Based System as a Function of Reaction Times[a]

| reaction time [s] | $\bar{M}_w \times 10^{-4}$ | $\bar{M}_w \times 10^{-4}$ | $\bar{M}_w/\bar{M}_n$ |
|---|---|---|---|
| 0.234 | 4.17 | 2.18 | 1.9 |
| 0.307 | 4.57 | 2.54 | 1.8 |
| 0.451 | 5.34 | 2.98 | 1.8 |
| 0.557 | 5.67 | 3.09 | 1.8 |
| 0.716 | 6.03 | 3.34 | 1.8 |
| 0.955 | 6.63 | 3.97 | 1.7 |
| 1.182 | 6.76 | 3.93 | 1.7 |
| 1.700 | 7.19 | 4.15 | 1.7 |
| 2,502 | 7.16 | 4.35 | 1.6 |
| 3.225 | 7.53 | 4.35 | 1.7 |
| 3.964 | 7.62 | 4.41 | 1.7 |
| 5.226 | 7.58 | 4.38 | 1.7 |

[a] $[Zr] = 9.52 \times 10^{-5}$ mol $L^{-1}$; $[Ph_3C][CN\{B(C_6F_5)_3\}_2] = 9.52 \times 10^{-5}$ mol $L^{-1}$; $[M]_0 = 0.59$ mol $L^{-1}$; 25.0 °C.

Again, assuming that $k_i \ll k_p$ and $k_t \ll k_p[M]_0$, we approximate this to

$$\langle n\rangle = \frac{\dfrac{k_p[M]_0}{k_t}\left[t + \dfrac{k_t}{k_i[M]_0(k_t - k_i[M]_0)}\left(e^{-k_i[M]_0 t} - 1\right) - \dfrac{k_i[M]_0}{k_t(k_t - k_i[M]_0)}\left(e^{-k_t t} - 1\right)\right]}{t + \dfrac{1}{k_i[M]_0}\left(e^{-k_i[M]_0 t} - 1\right)} \tag{10}$$

Applying the steady-state conditions with respect to both initiation and termination, that is, $\exp(-k_i[M]_0 t) \rightarrow 0$ and $\exp(-k_t t) \rightarrow 0$, reduces eq 11 further to

$$\langle n\rangle = \frac{k_p[M]_0 t}{1 + k_t t} \tag{11}$$

This form has been attributed to Natta and Pasquon[33] and has been widely used,[7−9] but it is not applicable here.[34]

(32) The influence of $k_i$ on the determination of the propagation rate constant $k_p$ is slight. For example, varying $k_i$ by a factor of 4 resulted in changes in $k_p$ of only about ≤10%.

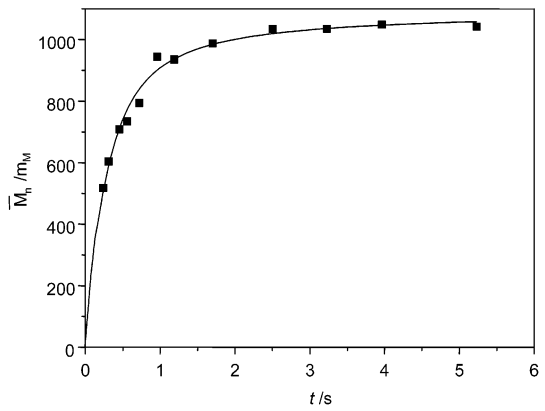


***Figure 7.*** Number-average degree of polymerization as a function of reaction time for the borate-based catalyst system. $[Zr] = 9.52 \times 10^{-5}$ mol $L^{-1}$; $[M]_0 = 0.59$ mol $L^{-1}$; $T = 25.0$ °C.

***Table 3.*** Polymer Yields $Y$ and Molecular Weights for MAO-Activated *rac*-(SBI)$ZrCl_2$ Catalyst[a]

| $t$/s | $Y$/g | $\bar{M}_n$ | $\bar{M}_w/\bar{M}_n$ |
|---|---|---|---|
| 2.281 | 0.0075 | | |
| 2.933 | 0.0110 | | |
| 3.913 | 0.0158 | 9530 | 1.7 |
| 4.844 | 0.0184 | 9470 | 1.7 |
| 6.966 | 0.0351 | 11 800 | 1.8 |
| 10.250 | 0.0695 | 13 500 | 1.7 |
| 13.215 | 0.0945 | 15 500 | 1.7 |
| 16.241 | 0.1146 | 15 600 | 1.7 |
| 21.419 | 0.1774 | 15 200 | 1.7 |

[a] $[Zr] = 1.46 \times 10^{-4}$ mol $L^{-1}$; $[M]_0 = 0.42$ mol $L^{-1}$; 40 °C. $Y$ = mass of polymer collected from 82 mL of effluent, corresponding to an input of 0.034 mol of propene.

Using eq 10 and the data shown in Figure 7, we obtain $k_t = 9.4 \pm 0.7$ $s^{-1}$ and an observed propagation rate $k_p[M]_0 = (10.1 \pm 0.8) \times 10^3$ $s^{-1}$, that is, $k_p = (17.2 \pm 1.4) \times 10^3$ L $mol^{-1}$ $s^{-1}$. The curve fitting is rather insensitive to the value of $k_i$, but least-squares calculations with starting values for $k_i[M]_0$ in the range of 1−5 $s^{-1}$ converged on a value of $k_i[M]_0 = 1.5 \pm 1.9$ $s^{-1}$, with $k_i \approx 2.5 \pm 3.2$ L $mol^{-1}$ $s^{-1}$, in satisfactory agreement with the value determined from the $Y(t)$ data.

**Methylalumoxane-Activated Catalysts.** It was of interest to compare the results from the borate-based catalyst system, $(SBI)ZrMe_2$/TIBA/$[Ph_3C][CN\{B(C_6F_5)_3\}_2]$, with the methylalumoxane-activated catalyst, *rac*-$(SBI)ZrCl_2$/MAO (Al/Zr = 2400:1). The productivity of the MAO system is lower, and, to obtain sufficient amounts of polymer, the reaction temperature was raised to 40 °C, the catalyst concentration was increased to $1.46 \times 10^{-4}$ mol $L^{-1}$, and the flow rate was reduced to 10.25 mL $min^{-1}$.

The experimental results are given in Table 3. The time-dependence of polymer yield (Figure 8) shows a shape very

(33) Natta, G.; Pasquon, I. *Adv. Catal.* **1959**, *11*, 1.
(34) Trial calculations with typical parameters show that eqs 10 and 11 agree well only when $\langle n\rangle$ has developed beyond 90% of the limiting value. For data which are predominantly within the range 50−90%, fitting to eq 11 can give values of $k_p$ which are in error by up to a factor of 2. The limiting value $k_p[M]/k_t$ is, however, quite well defined.

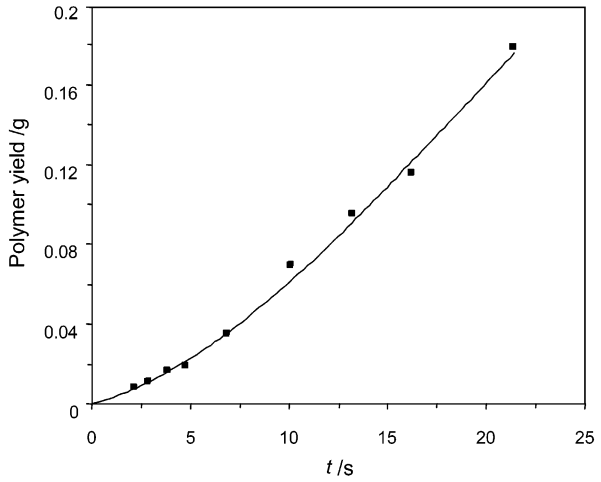


***Figure 8.*** Time-dependence of polymer yield in the system (SBI)$ZrCl_2$/MAO.

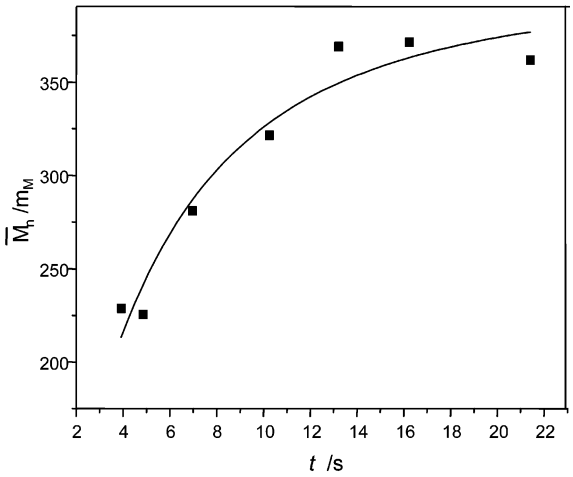


***Figure 9.*** Time-dependence of polymer molecular weight in *rac*-(SBI)-$ZrCl_2$/MAO catalyzed propylene polymerization. [Zr] = $1.46 \times 10^{-4}$ mol $L^{-1}$; $[M]_0 = 0.42$ mol $L^{-1}$; $T = 40$ °C.

similar to that of the borate-activated catalysts (Figure 4), although the time scale is longer. Analysis according to eq 5 gave $k_p = 48 \pm 3$ L $mol^{-1}$ $s^{-1}$ and $k_i \cong 0.25 \pm 0.05$ L $mol^{-1}$ $s^{-1}$.

The reaction-time-dependence of the number-average molecular weight of the MAO-activated system is shown in Figure 9. The trend resembles that in the borate system, although the limiting molecular weight is lower, $\bar{M}_n \approx 1.5 \times 10^4$ g $mol^{-1}$. In line with the slower reaction rate, this value is only reached after ca. 15 s. Curves fitted to eq 10 resulted in $k_p = 600 \pm 230$ L $mol^{-1}$ $s^{-1}$ and $k_t = 0.6 \pm 0.2$ $s^{-1}$, but no definite value of $k_i$ ($k_i \approx 0.8 \pm 2.6$ L $mol^{-1}$ $s^{-1}$).

**Effect of Counteranion Concentration.** The commonly accepted polymerization mechanism postulates cationic metal complexes as active species that are formed by dissociation of loosely coordinated anions.[2,3] If this is true dissociation, it should be detectable by the retarding effect of added common anion. "True dissociation" here means that some of the anions move out of the solvent cage reversibly and at a rate comparable to the rate of propagation, and of course the same would apply to the added salt. Contrary factors discussed by Brintzinger et al. are increased ionic strength due to added salt and also, in low-polarity solvents, the participation of ion multiples, either of which would tend to enhance the rate.[16,35]

***Scheme 5***

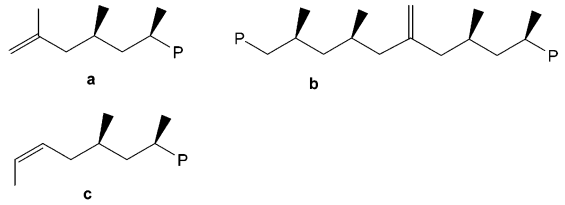


Observations on this point reported in the literature are apparently contradictory. For example, Schrock and co-workers found that in the living 1-hexene polymerization system [($^t$BuNON)$ZrMe^+\cdots B(C_6F_5)_4^-$] the addition of excess catalyst activator $[Ph_3C][B(C_6F_5)_4]$ strongly suppressed the polymerization, the rate constant falling from 9.2 to 3.8 L $mol^{-1}$ $min^{-1}$ with 1 additional equiv of trityl salt, which they attributed to the effect of the common anion $[B(C_6F_5)_4]^-$.[36] On the other hand, Landis found that in the system *rac*-$C_2H_4(Ind)_2ZrMe_2$/$B(C_6F_5)_3$ at 0 °C, also polymerizing 1-hexene, the addition of 1−4 equiv of $[PhNMe_3][MeB(C_6F_5)_3]$ had no influence on the rate.[10b]

We have found that, in the present system, adding $[PhCH_2N(C_2H_5)_3]^+[B(C_6F_5)_4]^-$ up to borate/Zr ratios of 20:1 had essentially no effect on the polymerization rate.[37] This finding is in agreement with the report by Landis on the effect of added $[MeB(C_6F_5)_4]^-$.[10b] On the other hand, the addition of incremental amounts of $[Ph_3C][B(C_6F_5)_4]$ had a positive effect and led to an increase in the rate of propene polymerization, up to a $CPh_3^+$/Zr ratio of 3:1. Further additions had little effect. These findings mirror earlier observations in batch reactions.[38,39] The chemical origin of this effect is not clear; further studies of this aspect are in progress.

**Misinsertion.** As pointed out in the Introduction, the lack of reactivity of *sec*-alkyl zirconocenes formed by propene 2,1-insertion can tie up a significant proportion of catalyst (Scheme 2, species **D4**), even though these regioerrors are rare.[40] As noted above, in the present system, the limiting $\bar{M}_n$ value is reached in only 0.1 s. The $^{13}C$ NMR spectrum of a polymer sample collected after a reaction time of $t = 0.95$ s showed ca. 0.1−0.2 mol % 2,1-regioerrors, that is, one in every 500−1000 insertions. Given the rate of growth, 2,1-misinsertions must therefore be considered as an important contributor to the dormant state concentration even at very short reaction times.

This picture was supported by polymer end-group analysis. The sample with $t = 0.95$ s showed three types of olefinic groups, **a**−**c** (Scheme 5). The vinylidene end-group **a**, formed by uni- or bimolecular $\beta$-H transfer and usually the most

(35) Beck, S.; Lieber, S.; Schaper, F.; Geyer, A.; Brintzinger, H. H. *J. Am. Chem. Soc.* **2001**, *123*, 1483.
(36) Goodman, J. T.; Schrock, R. R. *Organometallics* **2001**, *20*, 5205.
(37) Some batches of $[PhCH_2N(C_2H_5)_3][B(C_6F_5)_4]$ did suppress the reaction rate to varying degrees. This was traced to a borate impurity, most probably $[BrB(C_6F_5)_3]^-$ generated in the preparation directly from $BBr_3$. High purity $Li[B(C_6F_5)_4]$ was therefore made from $B(C_6F_5)_3$ and $LiC_6F_5$.
(38) Vathauer, M.; Kaminsky, W. *Polymer* **2001**, *42*, 4017.
(39) A reviewer suggested inefficient catalyst activation as a likely cause. However, the same effect was found in batch reactions with our catalyst system at longer reaction times (5 min, 20 °C), that is, under conditions where any time delay due to catalyst initiation is negligible as compared to the polymerization time.
(40) (a) Corradini, P.; Busico, V.; Cipullo, R. *Makromol. Chem., Rapid Commun.* **1992**, *13*, 21. (b) Busico, V.; Cipullo, R.; Coradini, P. *Makromol. Chem., Rapid Commun.* **1992**, *14*, 97.

*Scheme 6*

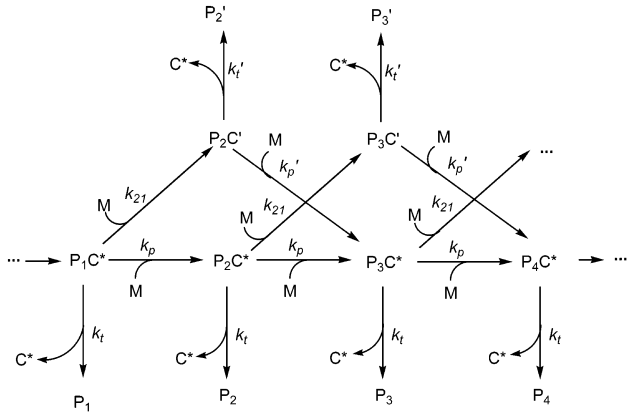


common end group, was only found in 24%. The internal vinylidene moiety **b** (10 mol %) has been explained by the intermediacy of a zirconium $\eta^3$-allyl complex, a product of C−H activation of a vinylidene-terminated chain.[41] Such a process would be expected to be relatively slow, and it was surprising to us to find evidence for **b** even in polymers prepared at such short reaction times. The most abundant end group, however, was the *cis*-butenyl structure **c** (66%) which results from a 2,1-regioerror followed by $\beta$-H elimination. Allylic or isobutenyl end groups or 1,3-enchainments were not found. The predominance of **c** shows that most chains are terminated following a 2,1-misinsertion.

To qualitatively allow for part of the active catalyst to be channeled into a resting state associated with 2,1-insertion, we propose the modified Scheme 6.

In this scheme, $P_zC'$ is a molecule with a regioerror adjacent to the catalytic center. In general, both $P_zC^*$ and $P_zC'$ may also have regioerrors in the body of the polymeryl chain, but these are not indicated in the scheme. $P_zC^*$ and $P_zC'$ together constitute the zirconium-bound polymer. Steps $k_{21}$ denote the misinsertions, and $k_p'$ denotes the 1,2-insertions following a regioerror. The scheme requires two terminations, $k_t$ and $k_t'$, both of which yield active forms of the catalyst as in Scheme 4, and we neglect any differences between these two active forms.

If we also neglect any chemical differences between polymers of different chain lengths and count all polymers $P_zC^*$ together as one species and all $P_z'C$ together as another, and also assume that termination is slow as compared to propagation, then $P_zC'$ and $P_zC^*$ can be considered to be in equilibrium. Thus, the ratio of molar amounts is given by $\sum_z[P_zC']/\sum_z[P_zC^*] = k_{21}/k_p'$, and the ratio of concentration of dead polymer formed by the two termination processes is approximately $(k_{21}/k_p')(k_t/k_t')$. As measured by the $^1$H NMR end-group analysis, this is 66/24 = 2.8.

At the time of quenching ($t \leq 5$ s), the mass of polymer isolated is derived mainly from metal-attached polymer chains, $mV\{\sum_z z[P_zC'] + \sum_z z[P_zC']\}$.[42] The observation that the rate of increase in mass with time is less than would be expected on the basis of the propagation rate deduced from molecular weight measurements is accounted for by supposing that, although the molar concentration of dormant Zr-polymeryl is greater than the molar concentration of active Zr-polymeryl (because $k_p'$ is small), the mass is less because the chains grow more slowly. The average chain lengths are $\langle n' \rangle = \sum_z z[P_zC']/\sum_z[P_zC']$ and $\langle n^* \rangle = \sum_z z[P_zC^*]/\sum_z[P_zC^*]$ for the dormant and active states, respectively, and our mechanism requires that $\langle n' \rangle$ is less than $\langle n^* \rangle$. Analysis of Scheme 6 in a steady-state approximation leads to $k_p/k_p^{app} = k_p(k_p' + k_{21})/k_p'(k_p + k_{21})$. With our assumptions that both $k_p'$ and $k_{21}$ are small as compared to $k_p$, this reduces to $1 + k_{21}/k_p'$, which was measured to be 12.9; hence, $k_{21}/k_p' \approx 12$.[43]

## Discussion

**Rate Law and Initiation.** The quenched-flow kinetic data for propene polymerization with both the borate-based and the MAO-activated catalyst systems are best in agreement with a mechanism that includes an initiation sequence as well as chain propagation as kinetically relevant steps at the early stages of the polymerization, as described by eq 4. In their studies on 1-hexene polymerization kinetics, Landis et al.[10] have developed a similar polymerization mechanism leading to the rate law of eq 12:

$$-\frac{d[M]}{dt} = k_p[M][C_0](1 - e^{-k_i[M]_0 t}) \qquad (12)$$

This differs from eq 4 in the preexponential factor. As a result, eq 12 gives an initial rate $(-d[M]/dt)_{t=0} = 0$, whereas eq 4 gives a finite value. The difference, however, is small, being due only to the amount of monomer consumed in the initiation step.

Our model shows $k_i$ as a second-order rate constant, in agreement with similar treatments in the literature.[9,10] Strictly speaking, although the reaction phase corresponding to initiation can be detected qualitatively, it is not possible to assign the order of reaction with respect to catalyst concentration on the basis of existing kinetic data.

The time scale of the initiation process implied by the kinetic measurements is similar to the time scale of the initial growth of the polymer as measured by the time-dependence of $\bar{M}_n$ (Figure 7); that is, we have $t_{1/2}^{init} = 0.24$ s, while the time for growth of polymer chains to one-half of the average final length is about 0.25 s. In other words, a high proportion of polymer growth takes place under non-steady-state conditions. Further progress in understanding this catalysis will depend on spectroscopic or other structural probes operating within these short time scales, and further work on this area is planned.

Several possibilities exist for the molecular processes involved in catalyst initiation. In catalysts based on metal−methyl complexes as precursors, the largest activation barrier is associated with the first monomer insertion to give a higher alkyl species $L_2Zr(CH_2CHMe_2)(X)$ (**1**, Scheme 7). On the other hand, as mentioned above, the system $(SBI)ZrMe_2/Al^iBu_3/[Ph_3C][CN\{B(C_6F_5)_3\}_2]$ generates a zirconocene isobutyl species **1**, that is, a complex where the alkyl ligand is identical to the

(41) (a) Resconi, R.; Piemontesi, F.; Camurati, I.; Sudmeijer, O.; Nifant'ev, I. E.; Ivchenko, P. V.; Kuz'mina, L. G. *J. Am. Chem. Soc.* **1998**, *120*, 2308. (b) Moscardi, G.; Resconi, L.; Cavallo, L. *Organometallics* **2001**, *20*, 1918.

(42) Determination of the end-group concentration by $^1$H NMR against 2-methoxynaphthalene as an internal standard in comparison with $\bar{M}_n$ determined by GPC has shown that, for $t \leq 5$ s, about 90% of the quenched polymer is saturated.

(43) A reviewer argued that it may not safe to assume that $k_t'$ is small as compared to $k_p'$. In that case, the estimate of $k_{21}/k_p' \approx 12$ would need to be revised upward.

***Scheme 7.*** Possible Formation and Structures of Active States **2** as the Result of Changes in Anion Coordination

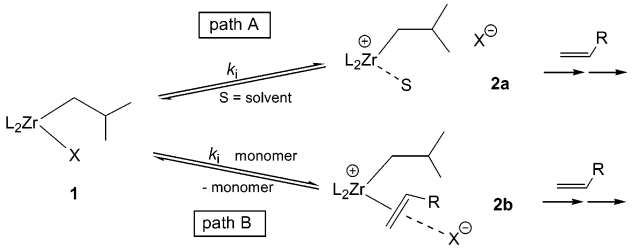


***Scheme 8.*** Anion Exchange-Assisted Monomer Insertion in Ion Aggregates

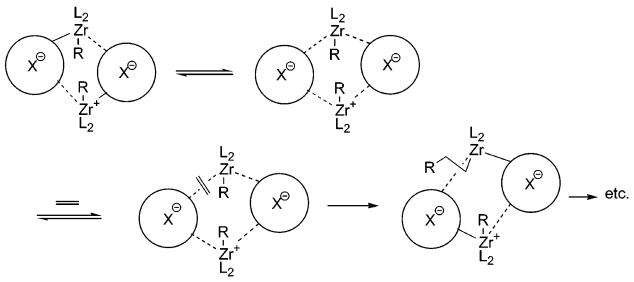


product of propene insertion into a Zr−Me bond. The first monomer insertion into such a Zr−$^i$Bu bond is therefore no longer rate-limiting, and in such a complex the first propene molecule should insert at about the same rate as subsequent insertions. We therefore consider that catalyst initiation is achieved by the displacement of the counteranion X from its coordination site in the contact ion pair, either to give a (possibly solvent-stabilized) ion pair **2a** which subsequently reacts rapidly with monomer or to undergo an associative anion substitution by the monomer to give a tight ion pair **2b**. Obviously, species **2a** and **2b** possess coordination sites suitable for monomer binding, whereas species of type **1** do not and are akin to a resting state. On the other hand, the absence of a rate-retarding anion concentration effect suggests that the anion remains within the ion pair solvent cage.

Recently, Brintzinger et al. determined the rate of anion exchange in zirconocene borate systems at 27 °C by NMR measurements. Various arguments supported the notion that the $[B(C_6F_5)_4]^-$ system exists in nonpolar solvents predominantly as ion quadruples or higher aggregates and that these provide a mechanism for anion exchange.[35] The apparent first-order exchange rate constants for the productive anion exchange of $[B(C_6F_5)_4]^-$ were estimated to be about 5000 times faster than those for $[MeB(C_6F_5)_3]^-$. For the $[(SBI)ZrMe^+\cdots B(C_6F_5)_4^-]$ system, they were on the order of 3000−12 000 $s^{-1}$ at the lower limit, very comparable to the monomer insertion rates observed here. It is tempting to hypothesize, therefore, that monomer uptake is coupled to anion exchange in such aggregates; in other words, anion exchange may provide a chemically plausible low-energy pathway for weakening the cation−anion interaction sufficiently to allow monomer binding to the metal center (Scheme 8).

**Active Species Concentration.** Knowledge of the concentration of species as a function of catalyst structure and/or the nature of the activator is a key to the understanding of catalytic systems. The increase in active species concentration [C*] as a function of time is given by eq 3b above. This describes the conversion of catalyst precursor into all of the species that have contributed to polymer production, that is, those zirconocenes carrying a polymeryl chain (eq 13).

***Table 4.*** Comparison of Kinetic Parameters for Trityl- and MAO-Activated Zirconocene Catalysts

| | (SBI)$ZrMe_2$/trityl[a] | | (SBI)$ZrCl_2$/MAO[b] | |
|---|---|---|---|---|
| | from $Y(t)$ | from $\bar{M}_n(t)$ | from $Y(t)$ | from $\bar{M}_n(t)$ |
| $k_p$, L $mol^{-1}$ $s^{-1}$ | 1320 ± 20 | 17 200 ± 1400 | 48 ± 3 | 600 ± 230 |
| $k_p^{obs}$, $s^{-1}$ | 780 ± 13 | 10 120 ± 800 | 20 ± 1 | 252 ± 97 |
| $k_i$, L $mol^{-1}$ $s^{-1}$ | 5.2 ± 0.6 | 2.5 ± 3.2 | 0.25 ± 0.05 | 0.8 ± 2.6 |
| $k_t$, $s^{-1}$ | | 9.4 ± 0.7 | | 0.6 ± 0.2 |
| ratio $k_p^{app}(Y)/k_p(M_n)$ | 0.08 | | 0.08 | |

[a] [Zr] = 9.52 × $10^{-5}$ mol $L^{-1}$, $[M]_0$ = 0.59 mol $L^{-1}$, 25.0 °C. [b] [Zr] = 1.46 × $10^{-4}$ mol $L^{-1}$; $[M]_0$ = 0.42 mol $L^{-1}$, 40.0 °C.

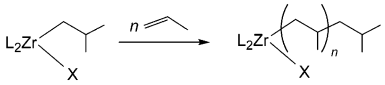


(13)

Over time − in this case about 2.5 s − the mole fraction of [C*] under this definition will approach 1.0. The value obtained by this method will therefore be similar to active species counts by isotopic quenching or labeling methods.[10,44]

However, the possibility of catalyst initiation by an anion displacement equilibrium implies a similar set of such equilibria between active and dormant states throughout the chain growth process. If one admits the intermittent growth model, our mechanism needs to be refined to take these equilibria into account (Schemes 7 and 8). While under such conditions almost all of the added catalyst precursor will contribute to polymer production over the duration of the reaction, only a small fraction is likely to be actively involved in the chain growth process at any one time. Under this definition, the term "active species" refers, for example, to the species depicted in box A of Scheme 2. Although this active fraction is obviously a determining factor of catalyst activity, it has proved difficult to estimate in metallocene catalysts and remains an unknown quantity for most systems.

The value of the propagation rate constant measured from the increase in the number-average polymer molecular weight as a function of time, $k_p \approx 17.2 \times 10^4$ L $mol^{-1}$ $s^{-1}$, is an order of magnitude higher than the $k_p$ value determined from the time-dependence of polymer yield at the same catalyst concentration. Relevant kinetic parameters are summarized in Table 4.

Determination of $k_p$ from eq 4 takes into account the total zirconium concentration, whether active or dormant; to avoid confusion, we will refer to the rate constant derived from $Y(t)$ as the apparent propagation rate, $k_p^{app}$. By contrast, the propagation rate derived from eq 9 is only concerned with the rate of growth of the polymer chain, irrespective of the number of metal centers involved. The ratio $k_p^{app}/k_p = 0.08$ for the trityl-activated catalyst suggests, therefore, that only about 8% of the total zirconocene concentration is involved in chain growth at any one time.[45]

Comparison to the (SBI)$ZrCl_2$/MAO catalyst is instructive. It was known from previous work that the MAO system was

(44) Chien, J. C. W.; Tsai, W. M. *Makromol. Chem., Macromol. Symp.* **1993**, *66*, 141.

(45) Following the suggestion by a reviewer, these figures may be adjusted taking into account catalyst loss due to unscavenged impurities, as estimated by the intercept in Figure 5b. This would raise the rate values for the trityl system by about 18% and increase the $k_p^{app}/k_p$ ratio from 0.08 to 0.09.

about 30−40 times less active than the borate-based catalyst.[19a] The limiting molecular weight, too, is much lower. Evidently, chain termination in the MAO catalyst is relatively more facile than that in the borate system, with $k_p[M]/k_t = 1086$ and 413 for borate and MAO, respectively.

At the outset of this investigation, we speculated that the difference in activities of the two systems might be due to the much lower concentration of active species in the MAO catalyst and that the actual rate of chain growth was dictated primarily by the structure of the metallocenium cation and essentially ligand-dependent, with little influence from the "weakly coordinating" anion, whether borate or [Me−MAO]$^-$. This argument was apparently supported by the negligible influence of the counteranion on the stereochemistry of polypropene that has been reported for some *ansa*-zirconocene catalysts.[46]

However, the kinetic data suggest a different scenario. For the MAO-activated system, $k_p^{app}/k_p \approx 0.08$; in other words, the percentage of active species in the MAO system is essentially identical to that found in the borate-based catalyst. On the other hand, $k_p$ for the MAO system is about 40 times smaller (Table 4). We have to conclude, therefore, that the counteranion profoundly influences the energetics of the migratory monomer insertion cycle. The equilibrium constant between an active species $[L_2ZrR(monomer)][X]$ and $L_2Zr(R)X$ (dormant state **D3**, Scheme 2) is apparently similar for either system. However, as shown in Scheme 2, the insertion process involves a series of successive products, and it appears that in the MAO system some of these have longer residence times, so that it takes much longer to follow the cycle through to its starting point. In effect, such comparatively long-lived intermediates can be considered as another type of (albeit unstable) dormant state; they differ, however, from states **D3** and **D4** in that they remain part of the chain growth sequence. The differences in $k_p$ measured for different activator systems also imply that the counteranion is closely associated with the cation throughout the insertion sequence, such as would be the case in a monomer-separated or solvent-separated ion pair.[47]

**The Nature of Dormant States.** As postulated above, the coordination site required for monomer binding prior to chain growth can, in principle, be made available by one of two processes. The anion might be envisaged to establish a dissociation equilibrium to give a solvent-separated ion pair, which subsequently binds the monomer (Scheme 7, path A), or the anion is displaced by the monomer in an associated substitution reaction but remains within the immediate vicinity of the monomer-stabilized metallocene cation (Scheme 7 path B and Scheme 8). The absence of a rate-retarding anion concentration effect is most in accord with the second scenario and suggests that the anion does not diffuse freely.

The polymer end-group analysis supported the notion that 2,1-misinsertions are a major source for the formation of dormant states. The model shown in Scheme 8 provided an estimate of $k_{21}/k_p'$. This has an interesting implication. As

***Scheme 9***

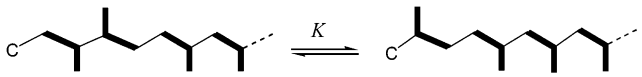


pointed out above, this is a measure of the equilibrium ratio between dormant and active states, but it can equally well be regarded as the equilibrium constant for the hypothetical methyl shift reaction at the head end of the polymeryl chain (Scheme 9). Assuming as before that the termination reactions do not significantly deplete the concentrations of dormant or active states, we found that our data gave the value $K = k_{21}/k_p' \approx 12$. This can be seen as a measure of the greater steric hindrance between a methyl adjacent to another methyl in the 2- and 3-positions of the polymeryl chain, as compared to the methyl group adjacent to the metallocene unit.

## Conclusion

The system $(SBI)ZrMe_2/Al^iBu_3/[Ph_3C][CN\{B(C_6F_5)_3\}_2]$ is a highly active catalyst for the polymerization of propene. The initial phase of the polymerization process has been studied using quenched-flow techniques under atmospheric pressure. Over the concentration range investigated, up to 1 bar of propene pressure, the reaction is first-order both in catalyst and in monomer. Curve fitting of the time-dependence of polymer mass gives an estimate of the rate of catalyst initiation, which for short reaction times is commensurate with the rate of propagation. A rate law taking account of these non-steady-state conditions has been proposed which confirms the absence of an induction period in these systems. At 25.0 °C, the observed propene insertion rate $k_p[M]$ is on the order of $10^4$ s$^{-1}$. The methylalumoxane-activated system $(SBI)ZrCl_2$/MAO shows very similar initiation and propagation behavior, but is about 40 times slower (at 40 °C). Comparison of the polymer mass data to the propagation rate constant obtained from the number-average molecular weight as a function of time provides an estimate of the fraction of total zirconocene that is actively engaged in the chain growth process at any one time. Surprisingly, this fraction is about the same for both the borate- and the MAO-based systems, ca. 8 mol %. While in an ion pair $[L_2ZrR]^+[X]^-$, where X is the noncoordinating anion, the rate of polymerization could be thought of as a function of the structure of the ligand L but independent of X, our results indicate that this is not the case. Monomer uptake and chain growth may be related to anion exchange processes, possibly via ion aggregates. The differences in propagation rates must mean that the counteranion strongly influences the residence times of one or more of the intermediates of the monomer insertion sequence, from monomer binding via $\gamma$- and $\beta$-agostically stabilized metal alkyls back to a species capable of monomer binding, which are much longer in the MAO system. In effect, these species may be regarded as a form of the dormant state, but they are different from nonproductive dormant states in that they are part of the chain growth cycle. These findings are in qualitative agreement with earlier batch results which provided a measure for the increase in the activation barrier of propene polymerization with anion basicity.[19] Propagation for the borate-activated system is ~6000 times faster than initiation. Analysis of the polymer microstructure indicates that even at short reaction times (≤1 s), 2,1-misinsertions and $\eta^3$-allyl zirconocene species are formed in kinetically relevant concen-

(46) (a) Herfert, N.; Fink, G. *Makromol. Chem., Rapid Commun.* **1993**, *14*, 91. (b) Hahn, S.; Fink, G. *Macromol. Rapid Commun.* **1997**, *18*, 117.

(47) The suggestion of close anion association within the active species gains further support by the observation of strong counteranion effects on the stereoselectivities and productivities of non-*ansa*-metallocene catalysts, notably Waymouth's oscillating $(2\text{-PhInd})_2ZrX_2$ system: (a) Wilmes, G. M.; Polse, J. L.; Waymouth, R. M. *Macromolecules* **2002**, *35*, 6766. (b) Busico, V.; Cipullo, R.; Kretschmer, W. P.; Talarico, G.; Vacatello, M.; van Axel Castelli, V. *Angew. Chem., Int. Ed.* **2002**, *41*, 505.

trations. These misinsertions are likely to be the main source for the ~90% of total [Zr] in reversibly dormant states. Tight ion pair formation may contribute to the dormant state concentration, but the extent of this contribution could not be quantified. The determination of the ratio $k_{21}/k_p'$ ratio from the concentration of 2,1-regioerrors allows the assessment of steric factors experienced by an incoming monomer. This parameter is likely to be strongly ligand-dependent; work to explore this aspect further is in hand.

**Acknowledgment.** This work was supported by the UK Engineering and Physical Sciences Research Council.

JA029150V